

Hybrid Position Controller for an Indirect Field-Oriented Induction Motor Drive

Antonio B. de Souza Junior; Tobias R. Fernandes Neto; Dalton de A. Honório; Luiz Henrique S. C. Barreto; Laurinda L. N. dos Reis

Robotic and Automation Research Group – GPAR / Department of Electrical Engineering / Federal University of Ceará

Centro de Tecnologia – Campus do Pici, Bl. 705

Fortaleza-CE, Brazil, 60455-760 / Phone: +55 85 33669586

E-mail: barbosa@dee.ufc.br, tobias@dee.ufc.br

Abstract—This paper presents a conception and implementation of a hybrid controller technique applied in an indirect field-oriented (FOC) induction motor drive. The main goal is to improve the position tracking performance with a hybrid controller based on the classical proportional (P) controller and the generalized predictive control (GPC) approach. It has shown through experimental results, the effectiveness of the proposed hybrid controller. Indeed, the controller has the fast tracking capability as a P controller and the robustness as a GPC controller.

I. INTRODUCTION

After the 1950s, the industrial automation field has been deeply researched. The advanced of microelectronics, semiconductor techniques and electrical machines are the main reasons of this. In fact, the induction machines (IM) are widely used in this area, because its low manufacturing cost, robustness and low maintenance need. However, IM has a non-linear mathematical model, which is closely dependent on the certainty of its parameters, e.g. rotor's resistance and inductance. When the application goal is the use of this kind of machine as a high-precision servo motor drive, this issue becomes an obstacle. Therefore, some modeling techniques were designed in order to overcome this barrier.

The FOC is one of them [1]. This technique allows modeling the IM similarly as a direct current (DC) machine. The machine variables effects can be decoupled due to a proper orientation of its magnetic fields, resulting in a simple model as an independent excited DC motor [2]. Thus, classical fixed gain controllers, like P and proportional-integral (PI), can be applied in the control loops of the IM, including the position loop. In general, there are two main performance requirements for motor drive applications: high disturbance rejection characteristics and the fast tracking of the set-point without overshoot [3]. Due to the need of high-precision applications, new approaches to obtain better results with the typical controllers are emerging.

Recently, structures mixing various types of controllers known as hybrid controllers have been proposed by several researchers in order to achieve the best performance for each

strategy. In [4], a hybrid PID controller is presented. The latter controller has the advantage of being easily tuned by a fuzzy controller, improving the system robustness. A new robust MRAC using a hybrid strategy is proposed in [5]. The implementation of a hybrid control for motor drive applications is proposed in [6]. This technique takes in count the power inverter state as a control variable in a switching-based hybrid system (HS), which is normally neglected by the classical control approaches.

In [7] a hybrid controller for robot manipulator is obtained by using the impedance control within the position controller and a variable structure model reaching control (VSMRC) in the force loop. The study made in [8] shows a hybrid speed control of a compound DC motor mixing a fuzzy controller with a proportional-integral-derivative (PID) controller. In the same line, [9] proposes a fuzzy hybrid controller for the position and force control loops, in order to reduce the number of sensors in an eye-to-hand robotic manipulator.

The paper deals with theoretical development and practical implementation of a hybrid position controller suitable for robotic applications, i.e., the use of IMs in the joint of a robot arm as a servomotor. The proposed controller mixes the advantages of two well known control techniques: the fast tracking response of the P controller and the robustness of the GPC controller. Therefore, experimental results will be depicted in order to demonstrate the main features of the developed system, to validate the employed methodology. The paper is organized as follows. Section II describes the mathematical model of the decoupled IM, as well as the proposed hybrid controller description in subsection controllers design. Section III presents the experimental setup and results. Finally, the conclusions are given in section IV.

II. MOTOR MODEL AND PROPOSED HYBRID STRATEGY

A. Motor Model

The FOC block diagram is shown in Fig. 1. The voltage source inverter (VSI), the space vector modulator and the control block with the position reference compose the system configuration. The SVPWM modulator converts the current

control signals in the specific switching functions for the VSI. The motor currents and the shaft position are used in its respective feedback loop.

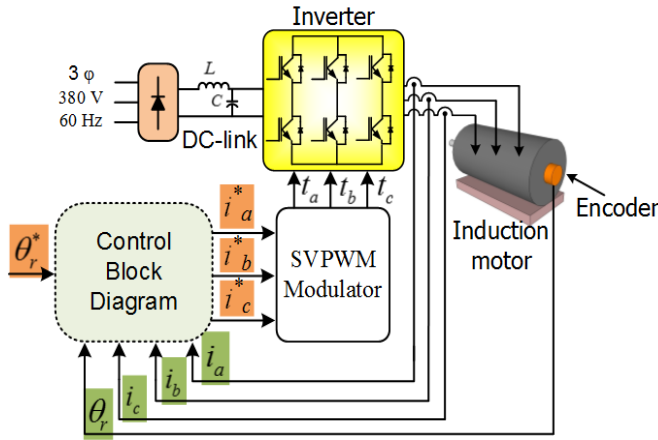


Figure 1. The field-oriented induction motor drive with the position control loop.

The state-space model of the induction motor in the rotating dq - reference frame is given as follows [2]:

$$\dot{x} = Ax + Bu \quad (1)$$

Where:

$$\dot{x} = \begin{bmatrix} i_{ds} \\ i_{qs} \\ \lambda_{dr} \\ \lambda_{qr} \end{bmatrix}; \quad B = \frac{1}{\sigma L_s} \begin{bmatrix} v_{ds} \\ v_{qs} \\ 0 \\ 0 \end{bmatrix};$$

$$A = \begin{bmatrix} \frac{R_s}{\sigma L_s} - \frac{R_r(1-\sigma)}{\sigma L_r} & \omega_e & \frac{L_m R_r}{\sigma L_s L_r^2} & \frac{P \omega L_m}{2 \sigma L_s L_r^2} \\ \omega_e & \frac{R_s}{\sigma L_s} - \frac{R_r(1-\sigma)}{\sigma L_r} & \frac{-P \omega L_m}{2 \sigma L_s L_r^2} & \frac{L_m R_r}{\sigma L_s L_r^2} \\ \frac{L_m R_r}{L_r} & 0 & \frac{R_r}{L_r} & \omega_e - \frac{P}{2} \omega_r \\ 0 & \frac{L_m R_r}{L_r} & -(\omega_e - \frac{P}{2} \omega_r) & \frac{R_r}{L_r} \end{bmatrix};$$

The electromagnetic torque T_e is given by:

$$T_e = \frac{3P}{4} \frac{L_m}{L_r} (i_{qs} \lambda_{dr} - i_{ds} \lambda_{qr}) \quad (2)$$

While expressions (3), (4), (5) give the following parameters:

$$\sigma = 1 - \frac{L_m^2}{L_s L_r} \quad (3)$$

$$\lambda_{qr} = L_m i_{qs} + L_r i_{dr} \quad (4)$$

$$\lambda_{dr} = L_m i_{ds} + L_r i_{qr} \quad (5)$$

In the field-oriented technique, the rotor flux linkage λ_r is assumed to be always aligned with the d -axis. Thus, the rotor flux linkage and its derivative in the q -axis is zero. Then, from (1) the d - and q - stator voltage equations are given in equations (6) and (7):

$$v_{qs} = \left(R_s + \left(L_s - \frac{L_m^2}{L_r} \right) s \right) i_{qs} + \omega_e L_s i_{ds} \quad (6)$$

$$v_{ds} = r_s i_{ds} - \omega_e \left(L_s - \frac{L_m^2}{L_r} \right) i_{qs} \quad (7)$$

The rotor flux linkage can be found from (1) and assuming that the magnetizing stator current i_{ds}^* will be kept constant, it is possible to obtain:

$$\lambda_{dr} = L_m i_{ds}^* \quad (8)$$

Then, rewriting (2) the electromagnetic torque is given by:

$$T_e = \frac{3P}{4} \frac{L_m^2}{L_r} i_{qs}^* i_{ds}^* \quad (9)$$

The variable i_{qs}^* represents the torque current command generated from the speed controller and the variable i_{ds}^* remains constant because of the fixed value of the rotor flux linkage in (8).

The slip angular speed ω_{sl} is necessary to calculate the rotor flux linkage angular position θ_e in the indirect FOC theory. Thus, with the equations (4) and (1), the slip angular speed is obtained:

$$\omega_{sl} = \frac{L_m R_r i_{qs}^*}{L_r \lambda_{dr}} = \frac{R_r i_{qs}^*}{L_r i_{ds}^*} \quad (10)$$

With the value of the slip angular speed and shaft position θ_r given by the encoder, it is possible to obtain the rotor flux linkage angular position:

$$\theta_e = \theta_r + \int \underbrace{\frac{R_r i_{qs}^*}{L_r i_{ds}^*}}_{\theta_{sl}} dt \quad (11)$$

The equation (11) proves the indirect field-oriented control. In other words, it is possible to obtain the position of the rotor flux linkage indirectly through the position of the machine shaft and the slip angle between the stator and rotor magnetic fields.

All this steps could be better visualized in Fig. 2, where the proposed hybrid control strategy is detailed.

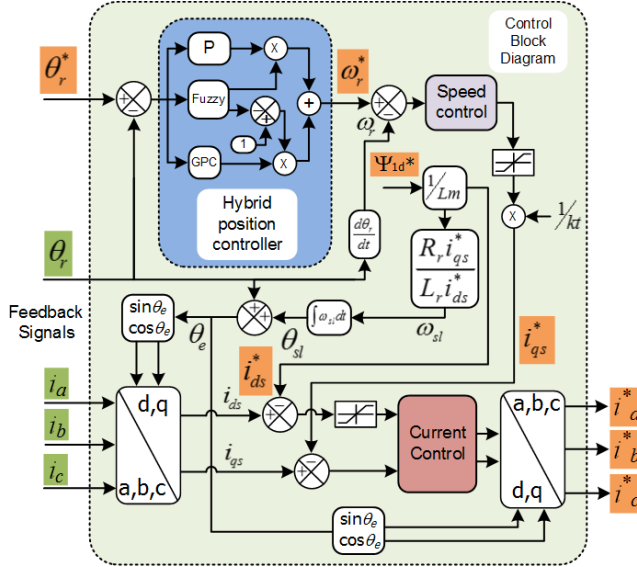


Figure 2. Control block diagram representing the indirect field-oriented induction motor drive with the position controller.

It could be noted that this kind of control approach is strongly dependent on the machine parameters, which may change during the motor running. Therefore, the control strategy must be robust enough against parametric uncertainties.

B. Proposed Hybrid Strategy

1) System modeling

In order to achieve a good performance from the controllers, it is necessary for the identification of the motor model. Then, it was approximated by a first-order plus time delay (FOPTD) model [10] and the chosen identification method was the Yuwana and Seborg[11]. From the step response shown Fig. 3, it is possible to extract the parameters needed to feed the model.

Using the Yuwana and Seborg[11] identification method with the acquired parameters, the position open loop transfer function in continuous-time was obtained and discretized by assuming a sampling rate of 0.1ms, resulting in:

$$H(z) = \frac{0.0008139z^{-1}}{1 - z^{-1}} \quad (12)$$

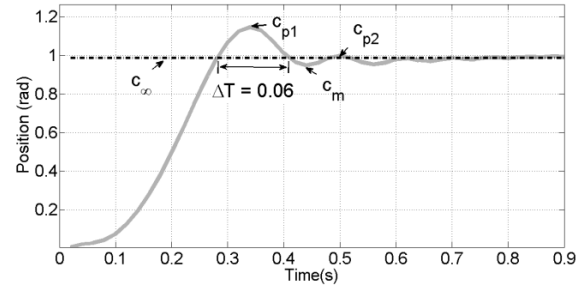


Figure 3. Step response using Yuwana and Seborg's method.

The Table I shows the acquired parameters.

TABLE I. PARAMETERS EXTRACTED FROM THE STEP RESPONSE OF THE YUWANA AND SEBORG IDENTIFICATION METHOD [11]

Method variables	Description	Value
c_{∞}	Steady state value	0.986 rads
c_m	Minimum of the output response	0.96 rads
c_{p1}	Fist peak of the output response	1.14 rads
c_{p2}	Second peak of the output response	1.01 rads
Δt	Half-period of oscillation	0.16

2) Proportional and GPC-Based I+P controllers design

The step response of the obtained transfer function model (12) is used in the Ziegler-Nichols tuning method [12]. As result, it was determined the parameter $K_p = 0.65477$ for the position controller. The others parameters for the current and speed controllers were calculated in [13].

The time-series model chosen for the predictive control is the Controlled Auto Regressive and Integrated Moving Average Model (CARIMA) [14]. The structure RST for the I+Pcontroller [12] was used, in order to obtain the GPC-Based I+P controllers, which is presented in Fig. 4. More details for the design and tuning method are presented in [15].

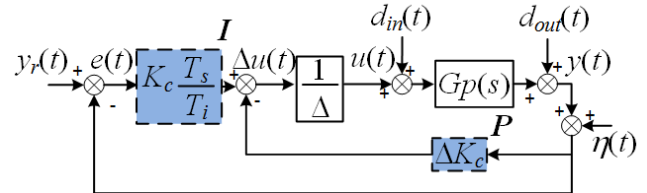


Figure 4. Proposed hybrid position controller block.

3) Structure of hybrid control using fuzzy logic

Fig. 5 shows with detail the proposed hybrid controller with fuzzy logic presented in Fig. 1. The action of two controllers can be weighted by the fuzzy algorithm. As it can be seen, there are two outputs for the fuzzy logic block: one is directly multiplied by the P block output, and the other one is

the complement of the first fuzzy output, then it is multiplied by the GPC block output. This complement is used, since the fuzzy logic typically employs values ranging from zero to one.

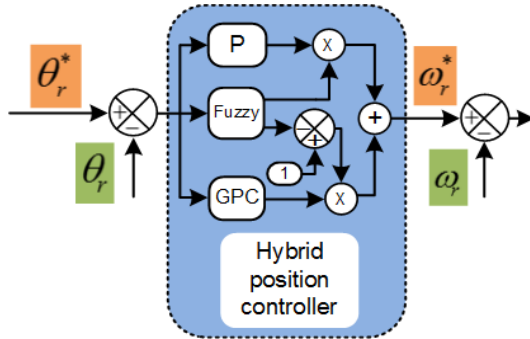


Figure 5. Proposed hybrid position controller block.

Table II shows the fuzzy rules used for the controller. As displayed, the behavior of the weighting fuzzy action applied to the P controller and the GPC controller, changes according to the position error. For instance, when the position error is 0.55, the fuzzy action will be 0.7 and the weighting of the P and GPC controllers will be 0.7 and 0.3, respectively, as shown in Fig.6.

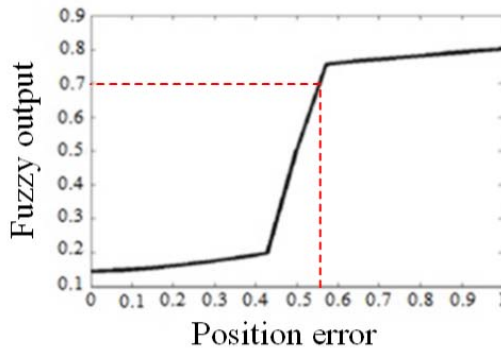


Figure 6. Fuzzy control surface.

The position error is calculated by difference of the reference position and the encoder position. The adopted linguistic rules express the relationship between the variables and they are defined as Positive Big (PB), Positive Medium (PM), Positive Small (PS), Zero (ZE), Negative Small (NS), Negative Medium (NM) and Negative Big (NB).

TABLE II. FUZZY RULES LOOP-UP TABLE

Position error	Fuzzy action	P controller weighting	GPC controller weighting
NB	PB	PB	PS
NM	PM	PM	PS
NS	PS	PS	PM
ZE	ZE	ZE	PB
PS	PS	PS	PM
PM	PM	PM	PS
PB	PB	PB	PS

In order to obtain the strategy combining both controllers, three different regions are developed from the control surface, which are called NARROW, P-GPC, and BROAD, as shown in Fig.7, where $e(\theta_r)$ is the normalized position error and μ is the membership degree.

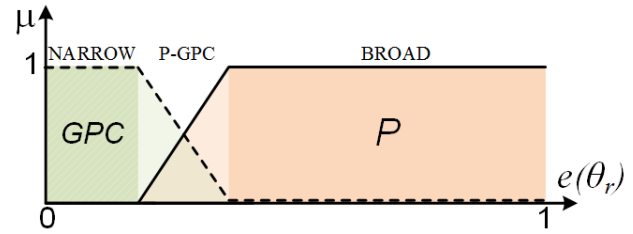


Figure 7. Membership functions used in fuzzy logic.

The first strategy involves a pure GPC region with little relevance relation. The output of this region aims to keep the steady-state error in a minimum value or eliminate it. The following region is the P-GPC, which produces a single output with both controllers. The purpose of this region is to smooth an eventual overshoot when the position reference suddenly is changed. The last area involves more the P action than the GPC, and it is responsible to bring the system to the reference as fast as possible.

III. EXPERIMENTAL SETUP AND RESULTS

A. Experimental Setup

One DSC from Texas Instruments® TMS320F28335 carries out the controller. The three-phase squirrel cage IM has four poles, 0.25HP and Y-connected windings. The specifications and parameters of the IM are given in Table III.

TABLE III. SPECIFICATION AND PARAMETERS OF THE IM

Rated Specifications		Motor's Parameters	
Rated power	0.25 HP	R_r	87.44 Ω
Rated speed	1725 rpm	R_s	35.58 Ω
Rated voltage	220 V	L_r	0.16 H
Rated current	1.26 A	L_s	0.16 H
Number of poles	4	L_m	0.884 H

The schematics and one photo of the experimental setup are shown in Fig.8 and Fig. 9, respectively. The inverter is a 10-kVA industrial voltage-source three-phase inverter from Semikron®. The mechanical load is a DC-motor from the manufacturer PHYWE®. The DSC produces a PWM switching frequency of 10 kHz and an incremental encoder, which is coupled to the motor shaft, gives the actual position. The DSC counter is used to count the encoder pulses and convert it to radians. The sampling time is 0.1ms. The current sensors are Hall-effect current sensor from LEM®.

B. Experimental Results

In order to verify the effectiveness of the implemented control strategy, several position tests are described. Four types of reference signals were utilized: step, sinusoidal, trapezoidal and triangular. The step reference verifies the controller's performance for an abrupt change in the position reference. The sinusoidal reference verifies the controller's performance when the position changes smoothly over the time. The trapezoidal reference checks the position tracking when the position increases linearly. The triangular reference verifies the abrupt position changing, when it reaches the maximum in either positive (or negative) direction.

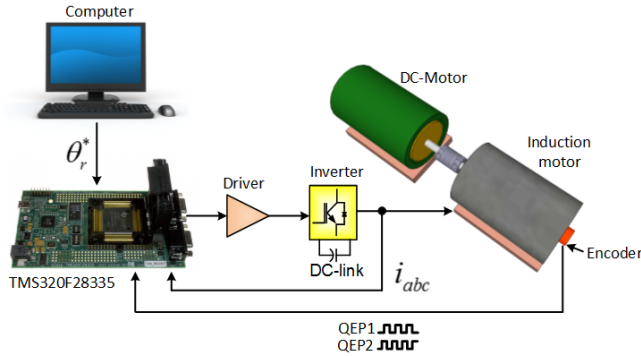


Figure 8. System's schematics.

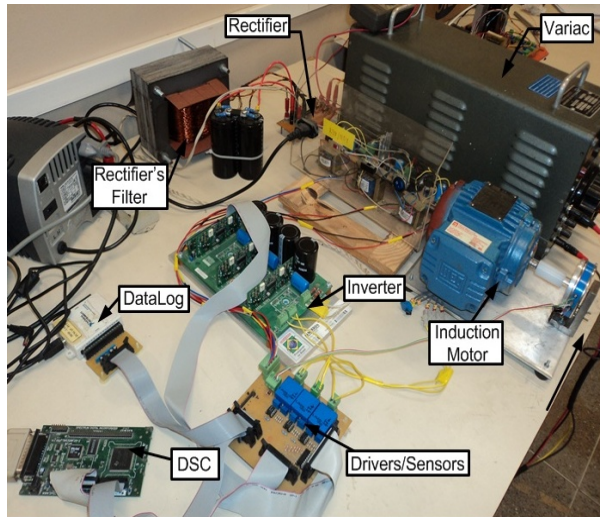


Figure 9. Experimental setup.

The first result is shown in Fig. 10, a step reference of 2rads is commanded in order to visualize the performance of each membership function of Fig. 7. In the interval $[t_0, t_1]$ the hybrid controller has the P action until the position error leaves the BROAD region. Afterwards, in $[t_1, t_2]$ the hybrid controller output is affected mainly by the P-GPC region. Finally, after t_2 the controller output is influenced by the NARROW region (GPC action), as much as the $e(\theta_r)$ is zero or nearly zero. Hence, it is possible to clearly visualize in the measured result the three dynamics of the proposed controller.

The next result is the system response for a sinusoidal reference position signal, which is shown in Fig. 11.

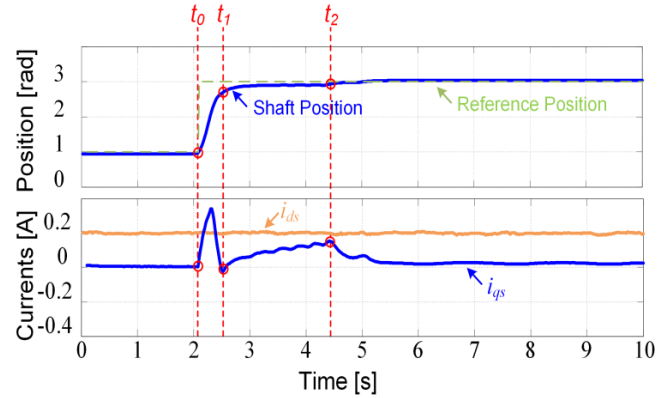


Figure 10. Experimental result for the system using a step position reference.

With this result, it is possible to note a good tracking characteristic of the reference signal. In the interval $[t_0, t_1]$ the controller acts like a mix of P-GPC, conducting the rotor of 3 rads to 1 rad steadily. The same response during the descending position in the interval $[t_0, t_1]$ is repeated during the ascending position in the interval $[t_1, t_2]$.

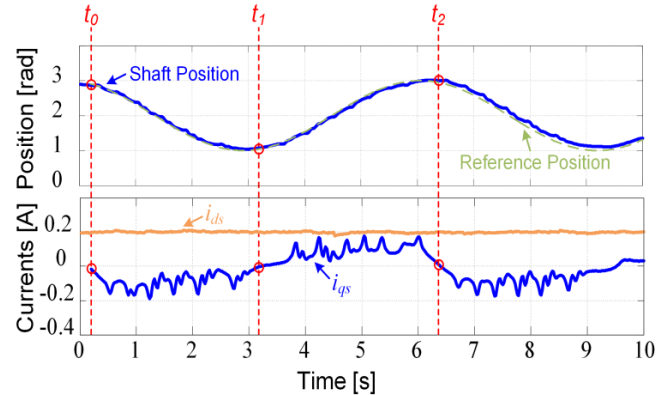


Figure 11. Experimental results for the system using a sinusoidal position reference.

The next result is the system response for a trapezoidal reference position signal. Fig. 12 shows the behavior of the shaft position and the currents i_{ds} and i_{qs} .

The intervals $[t_0, t_1]$ and $[t_2, t_3]$ have similar results. Therefore, the shaft position remained at stand still for the given reference value. On the other hand, in the interval $[t_1, t_2]$ and after $[t > t_3]$ the shaft position changes linearly, since the current i_{qs} is injected allowing the shaft rotation.

It can be noted in all results that the current i_{ds} remained constant in the reference value of 0.2A, proving the effectiveness of the d-axis current controller. The i_{ds} current is responsible for the magnetization of the machine and shall not be changed during the rotation of the shaft.

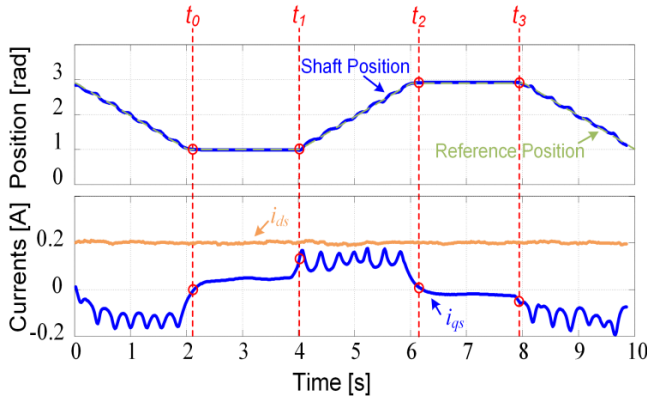


Figure 12. Experimental results for the system using a trapezoidal position reference.

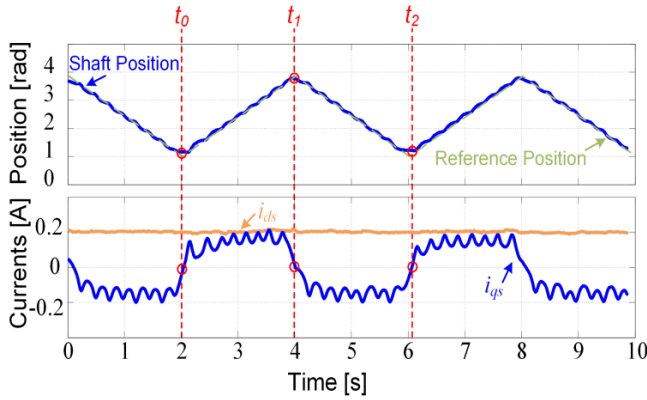


Figure 13. Experimental results for the system using a triangular position reference.

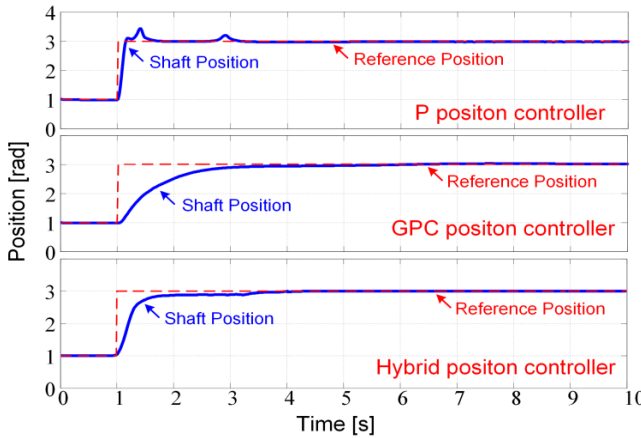


Figure 14. Experimental results for the comparison among P, GPC and Hybrid controllers.

Another result is shown in Fig. 13, where it is presented the system response for a triangular position reference signal. This test is similar to the result shown in Fig. 12, however, the controller has to provide the position reference tracking without a period of constant value. The latter result presents a good position tracking performance, even with the repetitive reference changes. Indeed, the behaviors depicted in the

intervals $[t_0, t_1]$ and $[t_1, t_2]$ are similar and with opposite directions, as expected.

The last result is shown in Fig. 14. It is a comparison of step responses of each controller individually. Each technique is tested alone in the position loop in order to analyze its performance and characteristics in contrast to the others. As it can be seen, the P controller has the faster settling time, nevertheless, with overshoot. For the GPC response, it noted the typical smooth settling motion with long periods. Finally, the proposed hybrid controller shows the good characteristics of both controllers alone in one single control structure.

IV. CONCLUSION

In this paper, it was shown an overview for a hybrid position controller used in an indirect field-oriented induction motor drive. Depending on the position error, the fuzzy logic block mixes both controllers actions (P and GPC) to achieve a fast and precise position tracking, and robust performance under load torque disturbance. With the given design procedures and the acquired test results, it can verify that the proposed control method is very robust and tolerates external system's uncertainties. Furthermore, this work shows the feasibility of the given position controller for embedded motor drive system. At last, this technique has proven to fulfill the requirements for robotic applications, e.g., the motor drive located at the joint of a robotic arm.

ACKNOWLEDGMENT

The authors would like to thank the CNPq and the CAPES for the financial support.

NOMENCLATURE

T_e	=	Electromagnetic torque, N.m
R_s	=	Stator resistance, Ω
L_s	=	Stator magnetizing inductance, H
R_r	=	Rotor resistance, Ω
L_r	=	Rotor magnetizing inductance, H
L_m	=	Magnetizing inductance, H
P	=	Number of poles
ω_e	=	Electrical angular speed, rad/sec
ω_r	=	Rotor angular speed, rad/sec
ω_{sl}	=	Slip angular speed, rad/sec
θ_r	=	Rotor angular position, rad
θ_e	=	Rotor flux linkage angular position, rad
θ_{sl}	=	slip angular position, rad
v_{ds}	=	d -axis stator voltage, V
v_{qs}	=	q -axis stator voltage, V
i_{ds}	=	d -axis stator current, A
i_{qs}	=	q -axis stator current, A
i_{ds}^*	=	d -axis stator current command, A
i_{qs}^*	=	q -axis stator current command, A
λ_{qr}	=	Rotor flux align with the q -axis, Wb
λ_{dr}	=	Rotor flux align with the d -axis, Wb
s	=	Laplace operator
z^{-1}	=	Backward shift operator
Δ	=	Differencing operator

REFERENCES

- [1] K. Hasse, *Zum dynamischen Verhalten der Asynchronmaschine bei Betrieb mit variabler Staenderfrequenz und Staenderspannung* ("On the dynamic behavior of induction machines driven by variable frequency and voltage sources"), *ETZ Arch.*, 1968, 89, pp. 77-81.
- [2] B. K. Bose, *Power electronics and AC Drives*, Prentice Hall PTR, Knoxville, 2001.
- [3] T. Ying-Yu, "DSP-Based robust control of an AC induction servo drive for motion control," *IEEE Transactions on Control Systems Technology*, vol. 4, no. 6, pp. 614-626, Nov. 1996.
- [4] T.-J. Ho, L.-Y. Yeh, "Design of a Hybrid PID Plus Fuzzy Controller for Speed Control of Induction Motors," *IEEE 2010 Conference on Industrial Electronics and Applications*, 2010, pp. 1352-1357.
- [5] K. Halbaoui, D. Boukhetala, F. Boudjema, "A new robust model reference adaptative control for induction motor drives using a hybrid controller," *IEEE 2008 International Symposium on Power Electronics, Electrical Drives, Automation and Motion*, 2008, pp. 1109-1113.
- [6] X. Lin-Shi, F. Morel, A. M. Llor, B. Allard, J. -M. Retif, "Implementation of Hybrid Control for Motor Drives," *IEEE Transactions on Industrial Electronics*, vol. 54, no. 4, pp. 1946-1952, Aug. 2007.
- [7] A. Jafari, J.-H. Ryu, M. Rezaei, R. Monfaredi, A. Talebi, S. S. Ghidary, "Sliding mode hybrid impedance control of robot manipulators interacting with unknown environments using VSMRC method," *2013 International Symposium on Robotics*, 2013, pp. 1-6.
- [8] J. Xiao, B. Li, D. Zhou, J. Chai, L. Zhang, "Speed Control System Based on Improved Fuzzy-PID Hybrid Control for Direct Current Motor," *2010 International Conference on Digital Manufacturing and Automation*, 2010, pp. 391-394.
- [9] W.-C. Chang, C.-K. Shao, "Hybrid fuzzy control of an eye-to-hand robotic manipulator for autonomous assembly tasks," *2010 Proceedings of SICE Annual Conference*, 2010, pp. 408-414.
- [10] L. A. Aguirre, *Introdução à Identificação de sistemas – Técnicas lineares e não-lineares aplicadas a sistemas reais*, Editora UFMG, Belo Horizonte, 2004.
- [11] M. Yuwana, D. E. Seborg, "A New Method for On-line Controller Tuning," *AIChE Journal*, vol. 28, no. 3, pp. 434-440, May 1982.
- [12] K. Åström, T. Hägglund, *PID Controllers Theory, Design and Tuning*, Instrument Society of America, Research Triangle Park, 1995.
- [13] D. A. Honório, E. C. Diniz, A. B. S. Júnior, O. M. Almeida, L. H. S. C. Barreto, "Comparison Between Sliding Model Control and Vector Control for a DSP-Based Position Control Applied to Squirrel-Cage induction Motor," *IEEE 2010 International Conference on Industry Applications*, 2010, pp. 1-6.
- [14] D. W. Clarke, "Generalized Predictive Control: A Robust Self-Tuning Algorithm," *1987 American Control Conference*, 1987, pp. 990-995.
- [15] A. B. de S. Júnior, E. C. Diniz, D. de A. Honório, L. H. S. C. Barreto, L. L. N. dos Reis, "Hybrid Control Robust Using Logic Fuzzy Applied to the Position Loop for Vector Control to Induction Motors," *Electric Power Components and Systems*, vol. 42, no. 6, pp. 533-543, Mar. 2014.